Intelligent Control Algorithm for Energy Management System of Light Electric Vehicles

FA Azidin[1], ZA Ghani[1], MA Hannan[2], M. Azah[2]
Faculty of Electronics and Computer Engineering (FKEKK)
Universiti Teknikal Malaysia Melaka (UTeM), Malaysia[1]
Department of Electrical, Electronic & Systems Engineering
Universiti Kebangsaan Malaysia (UKM), Malaysia[2]
faridarafat@utem.edu.my

***Abstract*—A state-based logic control algorithm was developed to coordinate a multi-source energy management system (EMS) for light electric vehicles (LEVs), such as scooters. This work was undertaken in view of the increasing importance of hybrid electric vehicles (HEVs) in many rapidly developing Asian countries. The multiple energy sources in this investigation were batteries, fuel cells (FC) and super-capacitors (SCs). Since each resource has its own advantages and disadvantages, a combination of the resources provides a more reliable and powerful energy model for hybrid electric vehicles (HEV). An algorithm was developed to manage the switching of the multiple energy resources efficiently. The performance of the proposed model in terms of vehicle acceleration and load power was measured against the ECE-47 test drive cycle. The sources of energy changeover were examined at 50% of the battery state of charge (SOC) or under heavy load conditions. The results showed a close match of the model to the test cycle under both normal and heavy load cycle conditions. The feasibility of the proposed intelligent controlling algorithm for the EMS of light electric vehicles was thus verified. This study could contribute huge benefit to the manufacturers and research institutions involved in light electric vehicle.**

***Index Terms*—fuel cell, battery, super-capacitors, control algorithm, energy management system.**

I. Introduction

Renewable energy is attracting more attention, especially for light electric vehicle (LEV) applications. Fuel cells, batteries and super-capacitors, with generated energy originates from renewable resources have potentially important roles in the development of an electric vehicle. For congested big cities, where small sized vehicles are preferable, electric vehicles provide many benefits. Much research has been carried out to improve the efficiency of such vehicles so that these vehicles use minimum energy as well as reduce emission.

Mulhall[1] carried out a novel study on an LEV, commonly known as the auto-rickshaw (three-wheel scooter) in Asia. The author proposed four different drive trains: a direct drive, a single electric motor, a parallel hybrid configuration, and a conventional drive with solar assist [2]. In that research, the last drive train system managed to improve electrical system efficiency by up to 77%. In another study of LEVs, Chao [3] described an FC electric scooter using field oriented control. Compared to the conventional scooter, the vehicle saved up to 43% of fuel and cost. Another innovation in the electric scooter was in the EMS for a direct drive vehicle [4]. In an energy efficiency test, the in-wheel electric scooter had a maximum battery to wheel up to 73.4%. The efficiency attained was almost the same as motor efficiency, with no additional losses in transmissions and differentials. Jia [5] studied FC-powered LEVs assisted by SCs, where a control mechanism managed the FC and SCs in a thermal balance system. Other studies related to EMS and HEV include that by Uzunoglu and Alam [6] who proposed a study on power sharing between FC and SCs using a control algorithm. The power converter system was driven by the PI controller to improve vehicle performance resulting in the 58 kW powered vehicle showing an improvement in energy saving. Salisa et al. [7] studied the Plug-in HEV (PHEV) that incorporated ADVISOR in MATLAB application. The study involved the distribution of the power system in EMS and the use of PID for vehicle propulsion control. The novel design of the power train configuration of the UTS PHEV gave better fuel economy and improved emission control [8]. Another study that involved an internal combustion engine (ICE)-PHEV was carried out by Song et al. [9]. The HEV, equipped with a dual-clutch transmission (DCT) and serial/parallel drive trains, achieved fuel saving of five percent. Vehicle energy storage components such as the battery and flywheel have been studied by Lukic et al. [10]. They also reviewed the electrical topology of EV and suggested a HEV classification with the EV categorized as 1 and the ICE vehicle as 0 [11]. Paper [12] proposed a novel design in energy management of batteries and SCs. The combined energy sources and an electric power train were developed in MATLAB/Simulink. The vehicle's performance which had a peak power of 32kW (300V) improved energy saving.

Although there have been comprehensive studies on batteries, FCs, and SCs, not much research has been carried out on the power sharing of these power sources for LEVs. Moreover, research in EV is normally focused on single-source, such as battery EV (BEV), Plug-in HEV (PHEV) and Fuel-cell vehicle (FCV) [13]. Multi-sources, which combined battery, FC and SC, is a new model of electric vehicle concept. These multi-sources, together with a control algorithm for the best power selection, are the major aspects of the present research. Thus, this could be a huge contribution in the development of electric vehicle.

II. Methods and System

There are three sources of energy used in the three-wheel LEV system: batteries, SCs and FC. The block diagram of the close loop system is shown in Figure 1. The EMS receives input signal from the control algorithm and activates the energy sources before it links to the motor drive system.

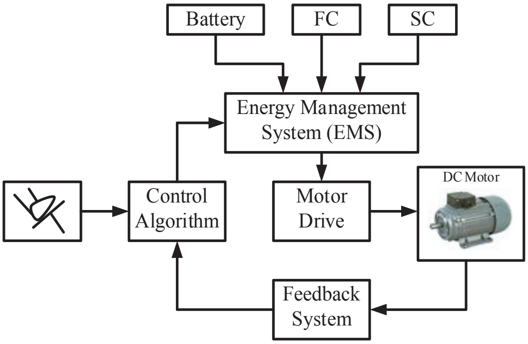

Figure 1: Multi-sources in a closed loop system for a LEV

A. Energy System Details

The battery model used in the system is set up as a controlled voltage source with an established V-I characteristics curve. The rechargeable and equivalent circuit of the battery model can be expressed as [14-15]

$$E = E_0 - K\frac{Q}{Q-it} + Ae^{(-B\cdot it)} \tag{1}$$

where, E and E_0 are the constant load and the no load voltage respectively, K is the polarized voltage constant, Q is the battery capacity, A is the exponential voltage, and B is the exponential capacity of the battery. The load current i and time t are parameterized respectively.

The battery V-I curve discharge increases due to the existence of internal resistance [16]. The load current has an inversely linear relationship to the SOC value. The discharge rate is calculated in [13-16] as follows:

$$SOC = 100*(1-\frac{Q*1.05}{\int i}) \tag{2}$$

The battery is empty when the SOC is 0% and fully charged at 100%. The established discharge characteristics curve of the battery in this system is shown in Figure. 2.

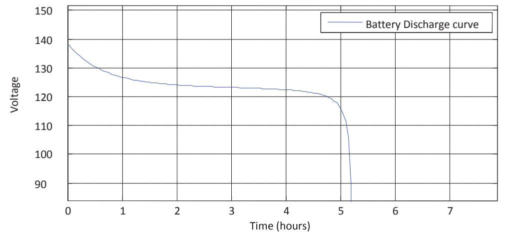

Figure 2: Battery current discharge characteristics at 0.2C (3A)

The FC model is designed by simplifying the previous model in [17]. A reaction between hydrogen and air produces energy, i.e. voltage [18]. The potential voltage E produced by the fuel cell is defined as

$$E = E_{OC} - NA_v \ln(i_{fc}) \tag{3}$$

where, E_{OC} is the open circuit voltage, N is the number of the cells, A_v is the exponential voltage, i_{fc} is the fuel cell current, and ln is the natural logarithm.

The FC is connected to the power diode to avoid reverse current flow to the system in a regenerative situation, and linked to the DC/DC converter to maintain a constant load voltage. The converter duty ratio for the switching period is controlled by the PI controller [16]. The duty ratio in terms of supply and load voltage is as follows [19]:

$$\frac{V_S}{V_L} = \frac{D}{1-D} \tag{4}$$

where, V_S is the supply voltage, V_L is the load voltage, and the D is the duty cycle. The V-I curve of the fuel cell model is presented in Figure 3.

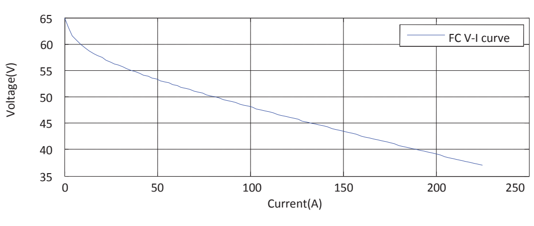

Figure 3: PEMFC simplified model V-I curve

The SC energy storage system is designed to aid the battery or FC, when there is high demand for power in the vehicle. The modeling of SC is related to the basic discharging circuit of the capacitor voltage in terms of the resistor and capacitor, i.e. the RC circuit. The effective discharging voltage depends on the initial voltage of the capacitor and the RC time constant, which is described in [20] as follows:

$$V_{SC}(t) = V_i e^{(-\frac{t}{RC})} \tag{5}$$

where, V_{SC} is the SC voltage and V_i is the initial voltage.

The amount of energy delivered by the SC is directly proportional to the capacitance and voltage changes throughout discharge, defined in [20] as follows:

$$E = \frac{1}{2} C (V_i^2 - V_f^2) \tag{6}$$

where, V_f is the final voltage and C is the capacitor value.

During charging and discharging, the capacitance and series resistance provide self-discharging losses that impact the long-term energy storage of the SCs. A number of SCs are arranged in series and parallel to provide a certain amount of energy during acceleration and peak load demand. The total resistance R_{total} and capacitance C_{total} of the SC module are calculated in [21] as follows:

$$R_{total} = n_s \frac{ESR}{n_p} \tag{7}$$

$$C_{total} = n_p \frac{C}{n_s} \tag{8}$$

where n_s is the number of capacitors in series, n_p is the number of capacitors in parallel, and ESR is the equivalent series resistance.

B. Energy Management System (EMS)

The EMS supervises the power sources to enhance the sharing of power before it is supplied to the load. The EMS system comprises the control algorithm, power control system, DC machine, and vehicle system. In the EMS of the LEV, the battery is the starting power source of the vehicle. When the start button is pushed, the processors determine the input condition, such as the battery capacity (BC), the pedal acceleration offset (PO), and the power demand (PD). Subsequently, the EMS determines which energy sources should be activated. This energy flow is illustrated in Figure 4. The main energy source, the FC, starts supplying energy to the load and recharges the battery when the battery capacity is below 50% (BC Low). If the battery reaches 80% of its capacity, the FC supply is cut off. The battery and FC share power if both the battery's capacity and load demand are high. The SC supplies energy to the load whenever the pedal offset is high.

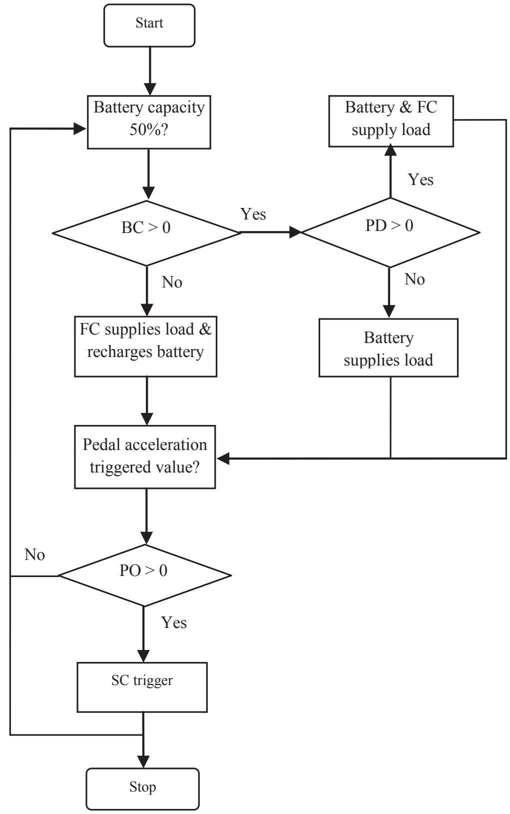

Figure 3: Flow process control of the LEV

C. Control Algorithm

A control algorithm is intended to achieve the condition based on the driving situation and to reduce energy consumption. The operational control strategies are based on the seven operation states shown in Table 1. The main task of the system is to supply sufficient power to drive the DC motor, depending on the power demand on the vehicle. The controller regulates three basic operational input conditions according to the battery capacity (BC), pedal offset (PO) and power duration load (PD); the latter two being determined by measuring the motor speed over a period of time. The control algorithm is defined by the control states in the logic combination shown in Table 1.

Table 1
Logic control algorithm in various conditions

State	SC	FC	Battery	Condition
1	0	0	0	Off operation/Safety features
2	0	0	1	BC-1; PD-0; PO-0
3	0	1	0	BC-0; PD-0; PO-0
4	0	1	1	BC-1; PD-1; PO-0
-	1	0	0	-- (Not possible)
5	1	0	1	BC-1; PD-0; PO-1
6	1	1	0	BC-0; PD-0; PO1
7	1	1	1	BC-1; PD-1; PO-1

Based on the source conditions, the seven operational states are as follows:

State 1: (Input: Safety Button): Off operation/safety features.

State 2: (Input: BC + /PD + /PO): Battery is fully used to drive the motor, if there is no high power demand. Part of the energy is conserved; the FC stays in operation and is active when the battery charge is low.

State 3: (Input: /BC + /PD + /PO): FC takes over to drive the vehicle and charge the battery until it turns to State 2.

State 4: (Input: BC + PD + /PO): The consequence of a high power demand forces the system to activate the FC as the auxiliary energy source.

State 5: (Input: BC + /PD + PO): In this situation, the battery-powered vehicle accelerates with the support of the SC. The vehicle, then turns to State 2 after all energy in the SC is used.

State 6: (Input: /BC + /PD + PO): The battery is critical. The FC-powered vehicle accelerates with additional energy from the SC. When the SC tank is empty, the system changes to State 3.

State 7: (Input: BC + PD + PO): As the vehicle moves into high speed and requires acceleration, the system is triggered to activate all of its energy sources.

In this system, the FC supply is unregulated, which means that there is full energy supply from the FC to the load. The system attempts to manage the operation of the energy sources based on the operational control strategy. Any excess energy will charge the battery because the FC and the battery are directly linked to each other.

D. Power Control System

All energy sources are linked to multi-switches, their activation being dependent on the input from the pedal acceleration (PO), battery SOC (BC), and high power demand load (PD). The detailed system that controls the switches and the current for the vehicle power load is shown in Figure 5. The supply current is the combination of currents from the battery, the FC, and the SC sources. The current is controlled by a PI controller that determines the reference current from the measured actual speed and the reference speed of the vehicle [15]. The reference current is then compared to an armature current to achieve the appropriate duty cycle for the DC chopper. The controlled current from the DC chopper provides the correct duty cycle that has been measured precisely to power the vehicle. In an H-bridge system, the switches are used to provide several modes of driving, such as forward drive, reverse drive, and motor braking. Because the analysis involves deceleration, the braking system comes from the current supply at the DC chopper.

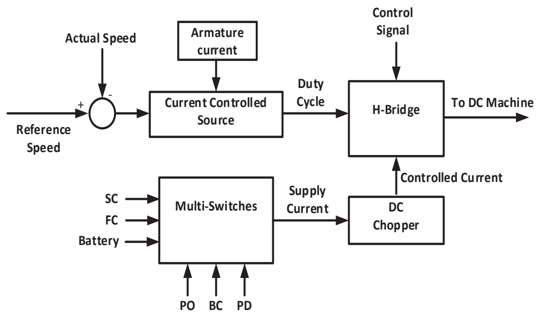

Figure 5: Power control system for a three-wheeled LEV

E. Power Control System

The vehicle system uses a separately-excited DC machine, where the same voltage supply is given at the field and the armature terminals. The induced counter electromotive force is proportional to the constant voltage and the electromechanical torque is proportional to the armature current multiplied by constant torque [22]. To convert the DC machine into a DC motor, multiplication of an input torque to the shaft and the electromechanical torque must be greater than zero. The parameters of the DC machine are presented in Table 2. The loaded power of the DC machine is calculated from the armature current and supply voltage.

Table 2
DC machine/motor parameters

DC Machine parameter	Values
Rated voltage, v (Field and Armature)	120 V
Armature resistance, R_a and Inductance, L_a	0.4382Ω, 0.006763 H
Field resistance, R_f and Inductance, L_f	84.91Ω, 13.39 H
Field armature mutual inductance, L_{af}	0.7096 H
Total Inertia, J	0.2053 kg.m^2
Viscous friction coefficient, B_m	0.007032 N.m.s
Coulomb friction torque, T_f	5.282 N.m

F. Vehicle System

The characteristics of the vehicle system of the LEV are shown in Table 3. The forces involved throughout the vehicle movement are the acceleration force, air friction force, wheel friction force, and slope friction force [22]. The power that moves the vehicle is calculated from the sum of the total forces multiplied by velocity [23].

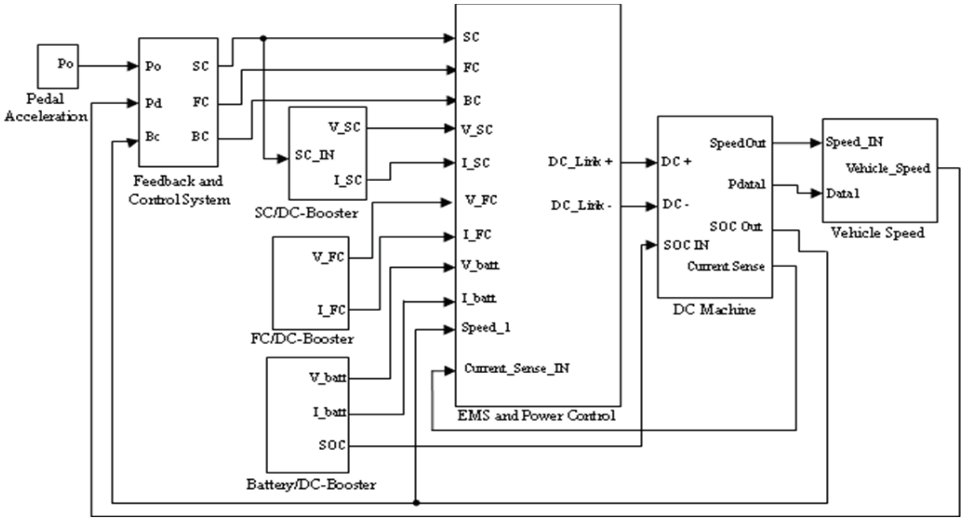

Figure 6: EMS and power control system block diagram

Table 3
Characteristics of the vehicle's dynamic parameters

Vehicle model parameter	Values
Tyre radius, *r*	0.26 m
Gear ratio, *G*	2.1
Vehicle mass + passengers	240 kg
Frontal Area, *A*	1.2 m^2
Drag coefficient, cd	0.75
Rolling coefficient, u_r	0.009
Air-density, *d*	1.25 kgm^{-3}
Gravity Acceleration, *g*	9.81 ms^{-2}

G. Program Structure

The development of the program structure starts by dimensioning the vehicle parameter, calculating the required DC machine, and choosing the specifications of the battery, FC and SC. The program structure is designed in block model in the MATLAB/Simulink. The structure of the simulation model (Figure 6) consists of three energy sources, switch, power control, DC machine/motor, vehicle system, and feedback and control system. The three energy sources are integrated in the switch and power control block, where all energy sources are controlled by switches that receive signals from the feedback and control system block. The selected output current is subsequently controlled by the PI regulator to control the speed following the drive cycle before it flows to the armature motor. The rated DC voltage with controlled current is connected to the DC machine, which converts the electrical energy into rotating speed. From the rotor speed, the vehicle speed is calculated according to mechanical transmission and vehicle parameters.

III. Results and Discussions

The performance of the LEV was investigated in terms of vehicle speed, power load, and multiple source loading conditions. The vehicle's performance was compared against the ECE-47 drive cycle, which is a standard European drive cycle for investigating the performance and emissions of mopeds and electric scooters. The trailing of LEV vehicle's speed and the drive cycle are shown in Figure 7. It is observed that the vehicle's speed and the ECE-47 test drive cycle were closely matched except during deceleration. The vehicle's system speed was controlled by the PI regulator, whereby a sudden change in speed could trigger a dampening response. It was evident that a few seconds were required to regulate the vehicle's speed until a constant speed was reached. The vehicle system started to break away from trailing the drive cycle at 55 s. When it reached a constant speed, over-braking and acceleration damping occurred before the system settled down at a constant speed. For the next deceleration test until the vehicle stopped, the dampening response rose again, and several seconds were needed to regulate the vehicle's speed until it stopped. According to the control algorithm, the vehicle system was in State 2. The LEV had no trouble following the drive cycle since the distance travelled was short, and the battery was sufficient to cope with the power demand. Obviously, the PI regulator would have to be more efficient to control vehicle's speed to avoid damping.

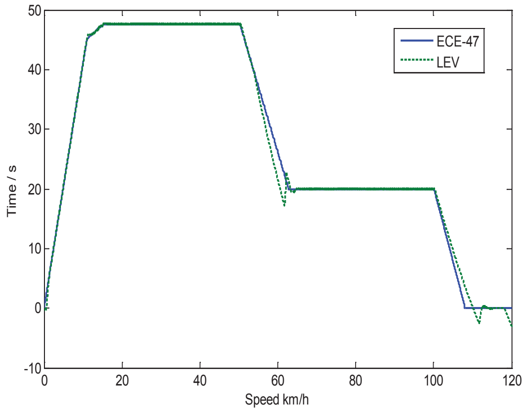

Figure 7: LEV in the ECE-47 test drive cycle

The measurement of the electrical power and the vehicle load power is presented in Figure 8. The average power required for the DC motor was 2.6 kW during vehicle acceleration for 18s. When the vehicle no longer accelerated, P_{elect} and P_{veh} remained at 1.5 kW. A reduction in the vehicle speed caused a dampening response in the P_{elect} due to the PI regulator. An electrical power spike was observed when the vehicle speed experienced over-braking, and there was a sudden demand for power to increase the vehicle's speed to the desired number of drive cycles. After 10 s, the system stabilized to an electrical power of 1.1 kW. The total energy consumed was estimated to be about 1.37 x 10^5 Ws.

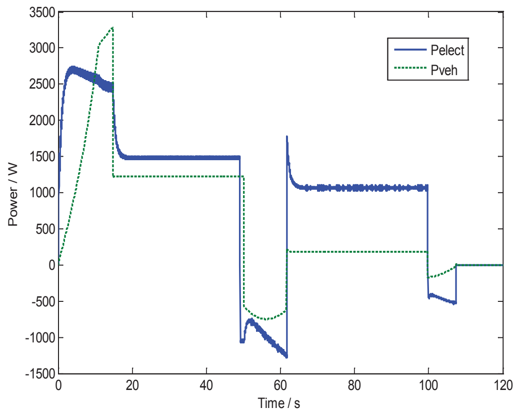

Figure 8: Vehicle and electrical power

The vehicle system condition was next investigated with the application of heavy load condition. The result of analysis is illustrated in Figure 9 with the LEV powered either by a single-source battery or a multi-source power input. It was observed that the performance of the multi-source LEV was superior to that of the single-source LEV in the first 18 s of acceleration. The single-source battery accelerated at 1.7 km /h/s, and reached a maximum speed of 43 km/h. In comparison, the multi-power system accelerated at about 2.35 km/h/s. The multi-source LEV managed a maximum speed that was slightly below the test drive cycle maximum speed of 47 km/h. The gap of the acceleration and maximum speed between the single-source and multi-source was hence quite significant. After 50 s of the drive cycle test, the vehicle started braking and reached a constant speed. Both the single and multi-source systems had the same deceleration path line and overshoot before reaching a constant speed. It was observed that when experiencing extreme power demand, the proposed EMS initiated the battery, the FC, and the SC to power the vehicle. At this stage, the control algorithm system was in State 7, subsequently returning to State 3 after the energy in the SC was exhausted. The vehicle's performance efficiency of the multi-source LEV was estimated to be about 95.7%, while that of the battery LEV was about 86.7%.

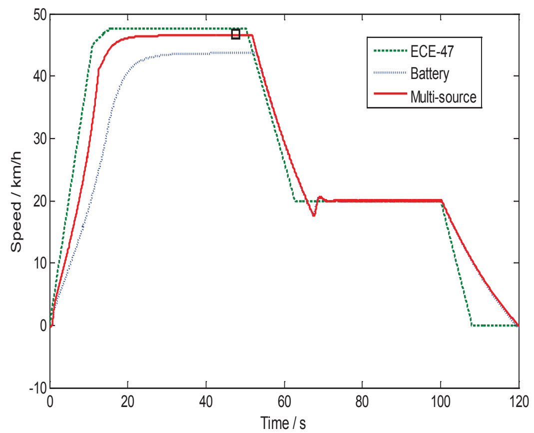

Figure 9: LEV in climbing stage in condition multi-source and single-source battery

The next test involved setting the SOC at 65% to observe the switching state from the battery to the FC. The battery current, the SOC and the FC current are shown in Figure 10. The speed drive cycle was similar to that in Figure 7. When the SOC reached 50% at 82 s, the battery turned off and the FC took over. At this stage, the system was in State 3 of the control strategy, where the FC supplied current to the motor and charged the battery at the same time. The vehicle continued to travel without any interruption at the point of switch-over, and there was no obvious indication when the changeover had occurred. Overall, the system conducted the switching without interrupting the power load supply.

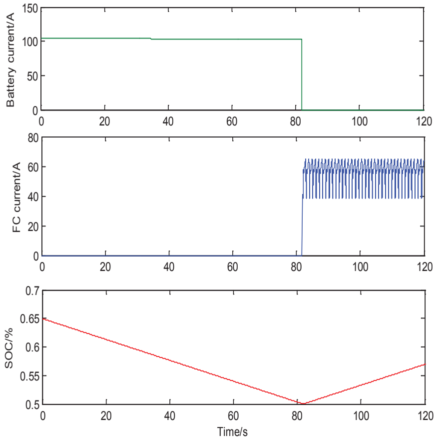

Figure 10: Battery current and SOC and FC current.

IV. Conclusion

This study encompasses an investigation on an alternative energy resource model for light class vehicles, such as the electric trishaw or scooter. In order to achieve the most efficient and reliable energy system for such vehicles, a combination of three resources: battery, FC, and SC was implemented. An intelligent switching algorithm that had the ability to control these multiple energy resources was developed as part of the EMS of the vehicle model. The algorithm was implemented based on seven different control states. These power resources took turns to act as primary and secondary resources based on the current vehicle acceleration, battery capacity, and vehicle load. The most challenging part in the implementation of the algorithm was the detection of the battery capacity and vehicle load, which had direct influence on the efficiency. To validate the proposed model and algorithm in terms of vehicle speed and load power, the developed EMS was tested against the ECE-47 test drive cycle under normal and heavy power demand conditions. The results showed that comparable performances were obtained under both driving conditions. The same result was also observed when the battery was at 50% capacity or undergoing heavy load conditions. This study hence showed that the controlling algorithm in the EMS improved efficiency and performance of the vehicle system.

Acknowledgment

The Authors would like to thank University Technical Malaysia Melaka (UTeM), National University of Malaysia (UKM), and Ministry Education of Malaysia (KPM) for financial support.

References

[1] P. Mullhall, S.G. Wirasingha, Y.J. Lee, A. Emadi, " Solar-Assisted Electric Auto Rickshaw Three-Wheeler," *IEEE Trans. Vehicular Technology,*; vol. 59(5): pp. 2298-2307, 2010.

[2] P. Mulhall, A. Emadi, "Comprehensive Simulations and Comparative Analysis of the Electric Propulsion Motor for a Solar/Battery Electric Auto Rickshaw Three-Wheeler," 35th *Annual Conference of IEEE on Industrial Electronics,* 2009, pp. 3785-3790.

[3] D. C.-H. Chao, P. J. v. Duijsen, J. J. Hwang, C.-H. Liao, "Modelling of a Taiwan Fuel Cell Powered Scooter," *International Conference on Power Electronics and Drive System,* 2009, pp. 913-919.

[4] Y.-P.Yang, J.-J. Liu, T.-H. Hu, "An Energy Management System for a directly electric scooter," *Journal on Energy Conversion and Management,* vol. 52 (2011), pp. 621-629, 2011.

[5] J. Jia, G. Wang, Y.T. Cham, Y. Wang, M. Han, "Electrical Characteristic Study of a Hybrid PEMFC and Ultracapacitor System," IEEE *Trans. on Industrial Electronics*, vol. 57 (6), pp.1945-1953, 2010.

[6] M. Uzunoglu, M.S. Alam, "Dynamic modeling, design and simulation of a PEM fuel cell/ultra-capacitor hybrid system for vehicular applications," Energy *Conversion and Management*, vol. 48(5), 1544-1553, 2007.

[7] A.R. Salisa, N. Zhang, J.G. Zhu, "A Comparative Analysis of Fuel Economy and Emissions between a Conventional HEV and the UTS PHEV," IEEE *Trans. Vehicular Technology*, vol. 60, pp. 44-54, 2011.

[8] A.R. Salisa, N. Zhang, J. Zhu, "Modeling and Simulation of an Energy Management System for Plug-in Hybrid Electric Vehicles," *Power Engineering Conference, AUPEC, 2008*, pp.1-6.

[9] Z. Song, W. Guangqiang, Z. Songlin, "Study on the Energy Management Strategy of DCT-based Series-Parallel PHEV," *International Conference on Computing, Control and Industrial Engineering,* 2010, vol.1, pp. 25-29.

[10] S.M. Lukic, J. Cao, R.C. Bansal, F. Rodriguez, A. Emadi, "Energy storage systems for automotive applications," *IEEE Transaction on Industrial Electronics*, vol. 55(6), pp. 2258-2267, 2008.

[11] S.M., Lukic, P. Mulhall, A. Emadi, "Energy autonomous solar/battery auto rickshaw," *Journal of Asian Electric Vehicles*, vol. 6(2), pp. 1135-1143, 2008.

[12] A. Jarushi, N. Schofield, "Modelling and Analysis of Energy Source Combinations for Electric Vehicles," *World Electric Vehicle Journal*, vol. 3, pp. 1-7, 2009.

[13] A. Khaligh, Z. Li, "Battery, Ultracapacitor, Fuel Cell, and Hybrid Energy Storage Systems for Electric, Hybrid Electric, Fuel Cell, and Plug-In Hybrid Electric Vehicles: State of the Art," *IEEE Trans. on Vehicular Technology,* vol. 59(6), pp. 2806-2814, 2010.

[14] L. Gao, Z. Jiang, R.A. Dougal, "An actively controlled fuel cell/battery hybrid to meet pulsed power demands," *Journal of Power Sources,* vol. 130, pp. 202-207, 2004.

[15] MathWorks, SimPowerSystems, *MATLAB*, 2008.

[16] P. Thounthong, V. Chunkag, P. Sethakul, B. Davat, M. Hinaje, " Comparative Study of Fuel-Cell Vehicle Hybridization with Battery or Super-capacitor Storage Device," *IEEE Trans. Vehicular Technology*, vol. 58(8), pp. 3892-3904, 2009.

[17] S. Basu, *Recent Trends in Fuel Cell Science and Technology*, New Delhi: Springer, 2007.

[18] H.J. Neef, "International overview of hydrogen and fuel cell research," Energy, vol. 34(3), pp. 327-333, 2009.

[19] L. Castaner, S. Silvestre, *Modelling Photovoltaic Systems Using PSpice*, New Jersey: John Wiley & Sons, INC., 2003.

[20] F.A. Azidin, M.A. Hannan, A. Mohamed, "An Energy Management of Light Electric Vehicle," *International Journal of Smart Grid and Clean Technology*, vol. 2(2), pp. 271-276, 2013.

[21] O.C. Onar, M. Uzunoglu, M. S. Alam, "Dynamic modeling, design and simulation of a wind/fuel cell/ultra-capacitor-based hybrid power generation system," *Journal of Power Sources,* vol. 161(1), pp.707-722, 2006.

[22] J. Larminie, J. Lowry, *Electric Vehicle Technology Explained*, West Sussex: John Wiley & Sons Ltd.; 2003.

[23] S.S. Williamson, A. Emadi, K. Rajashekara, "Comprehensive Efficiency Modeling of Electric. Traction Motor Drives for Hybrid Electric Vehicle Propulsion Applications," *IEEE Trans. on Vehicular Technology*, vol. 56(4), pp. 1561-72, 2007.